Asociación Argentina
de Mecánica Computacional

Mecánica Computacional Vol XXIX, págs. 5599-5611 (artículo completo)
Eduardo Dvorkin, Marcela Goldschmit, Mario Storti (Eds.)
Buenos Aires, Argentina, 15-18 Noviembre 2010

A HYBRID TIME/LAPLACE DOMAIN METHOD BASED ON NUMERICAL GREEN'S FUNCTIONS APPLIED TO PARABOLIC AND HYPERBOLIC BIOHEAT TRANSFER PROBLEMS

F.S. Loureiro[a], P. Oyarzún[a,c], J.P.L. Santos[a], W.J. Mansur[a], and C.A.B. Vasconcellos[b]

[a]*Department of Civil Engineering, COPPE/Federal University of Rio de Janeiro, CP 68506, CEP 21945-970, Rio de Janeiro, RJ, Brazil*

[b]*Department of Fortification and Construction Engineering, Military Institute of Engineering, Praça General Tibúrcio 80, CEP22290-270, Rio de Janeiro, RJ, Brazil*

[c] *Universidad Austral de Chile, Facultad de Ciencias de la Ingeniería, Instituto de Obras Civiles CP 567, CEP 5111187, Valdivia, Chile.*

Keywords: *Numerical Green's functions, FEM, Laplace domain, Bioheat.*

Abstract. There are some applications of extremely short time duration or at very low temperature for which the parabolic Pennes bioheat equation, which assumes an infinite thermal speed of propagation according to Fourier's law, is not adequate and the mathematical model may be more accurately described by the hyperbolic bioheat equation. Hence, the purpose of the present paper is to describe the numerical solution of both parabolic and hyperbolic bioheat equations in a unified manner by a hybrid time/Laplace domain method. Starting from the hyperbolic bioheat equation, which includes the parabolic one as a special case, the Explicit Green's Approach method that adopts numerical Green's function matrices in its formulation is employed to compute the solution on time. The Green's function equation is firstly discretized in the Laplace domain by the finite element method and then Green's function matrices are computed in the time domain through standard Laplace inversion algorithms. Finally, a numerical example is analyzed in order to illustrate the accuracy and potentialities of the proposed unified method.

1 INTRODUCTION

Numerical methods have been widely used as a powerful tool for the solution of many problems in the thermo-biology field. There are several different mathematical models that can be used to describe the bioheat transfer process in living tissue (Khanafer and Vafai, 2009). Among these, the Pennes' bioheat equation is frequently adopted in applications such as cancer hyperthermia therapies, cryosurgery, laser surgery, thermal diagnostics, skin burns and thermal comfort analysis. However, in some applications of extremely short time duration or at very low temperature (e.g., cryogenic surgery, laser-induced thermal damage, etc.) the mathematical model may be more accurately described by the hyperbolic bioheat equation, than the parabolic Pennes bioheat equation, which assumes an infinite thermal speed of propagation according to Fourier's law (Liu et al., 1999).

Green's functions are an important tool in solving partial differential equations since the solution of a problem subjected to any kind of initial conditions, boundary conditions and internal heat generation can be obtained through integral equations once the Green's function is known. Recently, a new methodology called Explicit Green's Approach (ExGA) was proposed by Loureiro (2007); Loureiro and Mansur (2010) to solve hyperbolic equations, e.g. the scalar wave equation; and later on the methodology was extended to solve parabolic equations (Mansur et al., 2009; Loureiro et al., 2009a); the authors applied the technique to the diffusion equation. The Explicit Green's Approach employs time-domain Green's function matrices to carry out the solution on time with its basic integral equation having some similarities with that of the time domain boundary element method. The key feature of the ExGA procedure stems from the fact that numerical Green's functions for bounded domains are used rather than analytical free-space Green's functions as in the standard time-domain boundary element methods. Thus, the ExGA can be easily applied to any kind of media, e.g., non-homogeneous, poroelastic, viscoelastic, anisotropic, etc.

The aim of this paper is to present a general time-domain formulation for the parabolic and hyperbolic bioheat equations by adopting a hybrid time-Laplace domain method developed by Loureiro and Mansur (2009b). In the proposed method, the Laplace transform in conjunction with the FEM is applied to the Green's function equation; subsequently, the Zakian Laplace inversion algorithm (Zakian and Edwards, 1978) is employed to compute the Green's function in the time domain with the final solution being obtained by means of a step-by-step time procedure. At the end of the paper, numerical results are presented to show the accuracy and potentialities of the proposed hybrid method.

2 BIOHEAT EQUATION

Let $\Omega \subset \Re^d$ be an open bounded domain with Lipschitz boundary $\Gamma = \partial\Omega$, where d is the number of space dimensions, and let $I = \left(0, t_f\right]$ be the time domain with $t_f > 0$, the governing equation concerning hyperbolic bioheat transfer problems reads (Liu et al., 1999):

$$\begin{aligned} &\nabla \cdot \left(k \nabla T\left(\mathbf{x},t\right)\right) + w_b c_b \left(T_b\left(\mathbf{x},t\right) - T\left(\mathbf{x},t\right)\right) + \\ &b\left(\mathbf{x},t\right) = \tau_r \rho c \ddot{T}\left(\mathbf{x},t\right) + \left(\rho c + \tau_r w_b c_b\right)\dot{T}\left(\mathbf{x},t\right) \end{aligned} \quad \text{in } \Omega \times I \tag{1}$$

where $b\left(\mathbf{x},t\right) = Q_m\left(\mathbf{x},t\right) + Q_r\left(\mathbf{x},t\right) + \tau_r\left(\dot{Q}_m\left(\mathbf{x},t\right) + \dot{Q}_r\left(\mathbf{x},t\right)\right)$.

In Eq. (1), ∇ denotes the gradient operator, $T_b\left(\mathbf{x},t\right)$ is the blood temperature and $T\left(\mathbf{x},t\right)$ is the tissue temperature, with over dots indicating derivatives with respect to time. Moreover, k, ρ and c stand for thermal conductivity, density and specific heat of tissue; c_b and w_b are the specific heat and perfusion rate of blood, respectively. The volumetric heat $b\left(\mathbf{x},t\right)$ contains the metabolic and spatial heating terms $Q_m\left(\mathbf{x},t\right)$ and $Q_r\left(\mathbf{x},t\right)$, as well as their time derivatives; τ_r is the thermal relaxation time of the biological system. The boundary Γ consists of a part Γ_1 with prescribed temperature and a part Γ_2 with prescribed heat flux, with its unit outward normal vector represented by $\mathbf{n}$, such that $\Gamma = \Gamma_1 \bigcup \Gamma_2$ and $\Gamma_1 \bigcap \Gamma_2 = \varnothing$, i.e.:

$$T\left(\mathbf{x},t\right) = \overline{T}\left(\mathbf{x},t\right) \text{ on } \Gamma_1 \times I \tag{2}$$

$$k \nabla T\left(\mathbf{x},t\right) \cdot \mathbf{n} = \overline{q}\left(\mathbf{x},t\right) \text{ on } \Gamma_2 \times I \tag{3}$$

In addition to the prescribed boundary values, initial conditions must be also specified as given below (the initial condition regarding the derivative of the temperature is normally set as null to correlate analyzes with the parabolic equation):

$$T\left(\mathbf{x},0\right) = T_0\left(\mathbf{x}\right) \text{ in } \Omega \tag{4}$$

$$\dot{T}\left(\mathbf{x},0\right) = \dot{T}_0\left(\mathbf{x}\right) \text{ in } \Omega \tag{5}$$

It is important to highlight that the heat flux obeys the modified Fourier's law according to the expression $\mathbf{q}\left(\mathbf{x},t\right) + \tau_r \partial \mathbf{q}\left(\mathbf{x},t\right)/\partial t = -k \nabla T\left(\mathbf{x},t\right)$ (Liu et al., 1999), which differs from the classical Fourier conduction law by an additional term including the time rate of change of the heat flux multiplied by τ_r. Furthermore, the well-known Pennes bioheat equation, which is of parabolic type, is readily obtained by assuming $\tau_r = 0$ in Eq. (1).

In this paper the solution for the bioheat equation is carried out by means of the Explicit Green's Approach developed by Loureiro (2007) and Loureiro and Mansur (2010) as discussed in the following section.

3 EXPLICIT GREEN'S FUNCTION APPROACH (EXGA) FORMULATION

This section is concerned with the application of the ExGA method to the bioheat equation in unified manner, where both parabolic and hyperbolic bioheat equations are solved from the same methodology by just setting the value of τ_r without any additional numerical consideration to accomplish each model.

3.1 Integral expression for the tissue temperature

In the ExGA formulation, the prescribed boundary condition on Γ_1 is firstly assumed to be satisfied exactly by splitting the temperature in the form $T(\mathbf{x},t)=\tilde{T}(\mathbf{x},t)+\hat{T}(\mathbf{x},t)$, where $\hat{T}(\mathbf{x},t)$ is a given function such that the condition $\hat{T}(\mathbf{x},t)=\overline{T}(\mathbf{x},t)$ on Γ_1 always holds. Afterwards, the weighted residual method is applied to Eq. (1) over the space-time domain, leading to the following integral identity:

$$\int_0^{t^+}\int_\Omega G(\mathbf{x},\mathbf{y},t-\tau)\begin{pmatrix}\nabla\cdot\left(k\nabla\tilde{T}(\mathbf{y},\tau)\right)+w_b c_b\left(T_b(\mathbf{y},\tau)-\tilde{T}(\mathbf{y},\tau)\right)+b(\mathbf{y},\tau)+\\ \psi(\mathbf{y},\tau)-\tau_r\rho c\dfrac{\partial^2\tilde{T}(\mathbf{y},\tau)}{\partial\tau^2}-\left(\rho c+\tau_r w_b c_b\right)\dfrac{\partial\tilde{T}(\mathbf{y},\tau)}{\partial\tau}\end{pmatrix}d\Omega_{\mathrm{y}}\,d\tau=0 \quad (6)$$

where $\psi(\mathbf{y},\tau)=\nabla\cdot\left(k\nabla\hat{T}(\mathbf{y},\tau)\right)-w_b c_b\hat{T}(\mathbf{y},\tau)-\tau_r\rho c\dfrac{\partial^2\hat{T}(\mathbf{y},\tau)}{\partial\tau^2}-\left(\rho c+\tau_r w_b c_b\right)\dfrac{\partial\hat{T}(\mathbf{y},\tau)}{\partial\tau}$.

In the present paper the Green's function $G(\mathbf{x},\mathbf{y},t-\tau)$ adopted as the weighting function in Eq. (6) satisfies the homogeneous boundary conditions of the original physical problem, with its governing equations being written as:

$$\begin{aligned}&\nabla\cdot\left(k\nabla G(\mathbf{x},\mathbf{y},t-\tau)\right)-w_b c_b G(\mathbf{x},\mathbf{y},t-\tau)+\delta(\mathbf{x}-\mathbf{y})\delta(t-\tau)\\&=\tau_r\rho c\ddot{G}(\mathbf{x},\mathbf{y},t-\tau)+\left(\rho c+\tau_r w_b c_b\right)\dot{G}(\mathbf{x},\mathbf{y},t-\tau)\end{aligned}\quad \text{in } \Omega,\ t>\tau \quad (7)$$

$$G(\mathbf{x},\mathbf{y},t-\tau)=0 \text{ on } \Gamma_1,\ t>\tau \quad (8)$$

$$k\nabla G(\mathbf{x},\mathbf{y},t-\tau)\cdot\mathbf{n}=0 \text{ on } \Gamma_2,\ t>\tau \quad (9)$$

where $\delta(\mathbf{x}-\mathbf{y})$ and $\delta(t-\tau)$ denote Dirac delta functions acting at the source point $\mathbf{y}$ and at time τ, respectively. Notice that due to the causality principle one has $G(\mathbf{x},\mathbf{y},t-\tau)=0$ and $\dot{G}(\mathbf{x},\mathbf{y},t-\tau)=0$ for $t<\tau$.

After making use of the Gauss divergence theorem and integration by parts, the basic ExGA integral expression for the temperature $\tilde{T}(\mathbf{x},t)$ reads (the reader is refereed to Loureiro et al. (2009a) and Loureiro and Mansur (2010) for further details):

$$\begin{aligned}\tilde{T}(\mathbf{x},t) = &\int_{\Omega} G(\mathbf{x},\mathbf{y},t)\,\rho c\tilde{T}(\mathbf{y},0)\,d\Omega_{\mathbf{y}} + \tau_r \int_{\Omega} G(\mathbf{x},\mathbf{y},t)\,w_b c_b \tilde{T}(\mathbf{y},0)\,d\Omega_{\mathbf{y}} \\ &+ \tau_r \int_{\Omega} \dot{G}(\mathbf{x},\mathbf{y},t)\,\rho c\tilde{T}(\mathbf{y},0)\,d\Omega_{\mathbf{y}} + \tau_r \int_{\Omega} G(\mathbf{x},\mathbf{y},t)\,\rho c\dot{\tilde{T}}(\mathbf{y},0)\,d\Omega_{\mathbf{y}} \\ &+ \int_0^{t^+}\int_{\Omega} G(\mathbf{x},\mathbf{y},t-\tau)\big(b(\mathbf{y},\tau) + w_b c_b T_b(\mathbf{y},\tau)\big)\,d\Omega_{\mathbf{y}}\,d\tau \\ &+ \int_0^{t^+}\int_{\Gamma_2} G(\mathbf{x},\mathbf{y},t-\tau)\,\bar{q}(\mathbf{y},\tau)\,d\Gamma_{\mathbf{y}}\,d\tau - \int_0^{t^+}\int_{\Omega} \nabla G(\mathbf{x},\mathbf{y},t-\tau)\cdot k\nabla\hat{T}(\mathbf{y},\tau)\,d\Omega_{\mathbf{y}}\,d\tau \\ &- \int_0^{t^+}\int_{\Omega} G(\mathbf{x},\mathbf{y},t-\tau)\,s(\mathbf{y},\tau)\,d\Omega_{\mathbf{y}}\,d\tau\end{aligned} \tag{10}$$

in which $s(\mathbf{y},\tau) = w_b c_b \hat{T}(\mathbf{y},\tau) + \tau_r \rho c \dfrac{\partial^2 \hat{T}(\mathbf{y},\tau)}{\partial \tau^2} + (\rho c + \tau_r w_b c_b)\dfrac{\partial \hat{T}(\mathbf{y},\tau)}{\partial \tau}$.

3.2 Spatial discretization and step-by-step time procedure

The main idea behind the ExGA method consists of the application of a discretezation methodology for the temperature field as well as for the Green's function in Eq.(10). Here, finite element discretization concepts are employed and both the temperature and the Green's function are approximated by piecewise polynomial basis functions N_i as:

$$\tilde{T}^h(\mathbf{y},\tau) = \sum_{l\in\eta-\eta_{\Gamma_1}} N_l(\mathbf{y})\,\tilde{T}_l(\tau) \tag{11}$$

$$\hat{T}^h(\mathbf{y},\tau) = \sum_{l\in\eta_{\Gamma_1}} N_l(\mathbf{y})\,\overline{T}_l(\tau) \tag{12}$$

$$G^h(\mathbf{x},\mathbf{y},t-\tau) = \sum_{j\in\eta-\eta_{\Gamma_1}} N_j(\mathbf{y})\,G_{kj}(t-\tau) \tag{13}$$

where η is the set of all nodes in $\bar{\Omega}$ and $\eta_{\Gamma_1} \subset \eta$ the subset corresponding to those nodes located on Γ_1.

After substituting approximations (11)-(13) into Eq. (10), the temperature integral expression for the discrete nodal values of $\tilde{T}(\mathbf{x},t)$ in the time domain can be represented in matrix form as:

$$\tilde{\mathbf{T}}(t) = \big(\mathbf{G}(t)(\mathbf{M}+\tau_r\mathbf{C}) + \tau_r\dot{\mathbf{G}}(t)\mathbf{M}\big)\tilde{\mathbf{T}}(0) + \tau_r\mathbf{G}(t)\mathbf{M}\dot{\tilde{\mathbf{T}}}(0) + \int_0^t \mathbf{G}(t-\tau)\mathbf{F}(\tau)\,d\tau \tag{14}$$

where $\mathbf{G}(t)$ and $\dot{\mathbf{G}}(t)$ represent the Green's function and its time derivative written in matrix form for the discrete system. The matrix and vector entries appearing in Eq. (14) are defined as:

$$M_{jl} = \int_{\Omega} N_j(\mathbf{y}) \rho c N_l(\mathbf{y}) d\Omega_{\mathbf{y}} \tag{15}$$

$$C_{jl} = \int_{\Omega} N_j(\mathbf{y}) w_b c_b N_l(\mathbf{y}) d\Omega_{\mathbf{y}} \tag{16}$$

$$\begin{aligned} F_j(\tau) = & \int_{\Omega} N_j(\mathbf{y}) \left(b(\mathbf{y},\tau) + w_b c_b T_b(\mathbf{y},\tau) \right) d\Omega_{\mathbf{y}} + \int_{\Gamma_2} N_j(\mathbf{y}) \overline{q}(\mathbf{y},\tau) d\Gamma_{\mathbf{y}} - \\ & \left(\int_{\Omega} \nabla N_j(\mathbf{y}) \cdot k \nabla N_l(\mathbf{y}) d\Omega_{\mathbf{y}} + \int_{\Omega} N_j(\mathbf{y}) w_b c_b N_l(\mathbf{y}) d\Omega_{\mathbf{y}} \right) \overline{T}_l(\tau) - \\ & \int_{\Omega} N_j(\mathbf{y}) \left(\rho c + \tau_r w_b c_b \right) N_l(\mathbf{y}) d\Omega_{\mathbf{y}} \frac{\partial \overline{T}_l(\tau)}{\partial \tau} - \tau_r \int_{\Omega} N_j(\mathbf{y}) \rho c N_l(\mathbf{y}) d\Omega_{\mathbf{y}} \frac{\partial^2 \overline{T}_l(\tau)}{\partial \tau^2} \end{aligned} \tag{17}$$

One should observe that the semi-discretization procedure carried out in Eq. (10) for which the spatial domain is discretized first and hence decoupled from the time domain gives rise to a simpler convolution integral dependent only in time. In this way, it is possible to replace the time dependent convolution integral by a particular solution related to the external heat load (Loureiro and Mansur, 2009b). Thus, Eq. (14) can be rewritten in terms of the particular solution as:

$$\tilde{\mathbf{T}}(t) = \left(\mathbf{G}(t)(\mathbf{M} + \tau_r \mathbf{C}) + \tau_r \dot{\mathbf{G}}(t) \mathbf{M} \right) \left(\tilde{\mathbf{T}}(0) - \tilde{\mathbf{T}}_p(0) \right) + \tau_r \mathbf{G}(t) \mathbf{M} \left(\dot{\tilde{\mathbf{T}}}(0) - \dot{\tilde{\mathbf{T}}}_p(0) \right) + \tilde{\mathbf{T}}_p(t) \tag{18}$$

where $\tilde{\mathbf{T}}_p(t)$ is the particular solution vector corresponding to the external heat load vector $\mathbf{F}(t)$ [xx] (the reasons for the adoption of the particular solution rather than the convolution integral are commented later).

Instead of applying Eq. (18) at each time level, a step-by-step time procedure is adopted to compute the solution. In the step-by-step time procedure the solution at the current time, say t_{k+1}, is computed from the previous known solution at time t_k. To do so, the first step is to obtain the expression for the derivative of the temperature vector by differentiating Eq. (18) with respect to time. Afterwards, the total time interval $\left[0, t_f\right]$ is split into N equal time intervals, i.e., $\left[0, t_f\right] = \bigcup_{k=0}^{N-1} \left[t_k, t_{k+1}\right]$ with $0 = t_0 < t_1 < \ldots < t_N = t_f$, $\Delta t = t_{k+1} - t_k = t_f / N$, $t_k = k\Delta t$ and $t_{k+1} = (k+1)\Delta t$. Finally, the below step-by-step expression arises after taking into account all the aforementioned procedures:

$$\begin{aligned}\tilde{\mathbf{T}}^{k+1} &= \left(\mathbf{G}\left(\Delta t\right)\left(\mathbf{M}+\tau_r\mathbf{C}\right)+\tau_r\dot{\mathbf{G}}\left(\Delta t\right)\mathbf{M}\right)\left(\tilde{\mathbf{T}}^{k}-\tilde{\mathbf{T}}_p^{k}\right)+\tau_r\mathbf{G}\left(\Delta t\right)\mathbf{M}\left(\dot{\tilde{\mathbf{T}}}^{k}-\dot{\tilde{\mathbf{T}}}_p^{k}\right)+\tilde{\mathbf{T}}_p^{k+1}\\ \dot{\tilde{\mathbf{T}}}^{k+1} &= -\mathbf{G}\left(\Delta t\right)\left(\mathbf{K}+\mathbf{C}\right)\left(\tilde{\mathbf{T}}^{k}-\tilde{\mathbf{T}}_p^{k}\right)+\tau_r\dot{\mathbf{G}}\left(\Delta t\right)\mathbf{M}\left(\dot{\tilde{\mathbf{T}}}^{k}-\dot{\tilde{\mathbf{T}}}_p^{k}\right)+\dot{\tilde{\mathbf{T}}}_p^{k+1}\end{aligned} \tag{19}$$

where $K_{jl}=\int_{\Omega}\nabla N_j\left(\mathbf{y}\right)\cdot k\nabla N_l\left(\mathbf{y}\right)d\Omega_{\mathbf{y}}$. Notice that for the Pennes equation (i.e., assuming $\tau_r=0$ in Eq. (19)) only the temperature expression is required to carried out the time marching process since the temperature time derivative vector does not appear in its expression.

Because the time step Δt is usually small compared to the total time of analysis, it is straightforwardly and acceptable in a great number of cases to assume a linear variation for the external heat load vector, i.e., $\mathbf{F}\left(t\right)=\mathbf{F}^{t}+\left(\mathbf{F}^{t+\Delta t}-\mathbf{F}^{t}\right)\tau/\Delta t$ ($\tau=t-t_k$ being the increase in time from the beginning of every time step $t_k=k\Delta t$ with $0\le\tau\le\Delta t$). Thus, according to this variation the particular solution reads $\tilde{\mathbf{T}}_p\left(t\right)=\boldsymbol{\varphi}_1+\boldsymbol{\varphi}_0\tau$, where the vectors $\boldsymbol{\varphi}_1$ and $\boldsymbol{\varphi}_0$ are computed as (Loureiro and Mansur, 2009b):

$$\begin{aligned}\left(\mathbf{K}+\mathbf{C}\right)\boldsymbol{\varphi}_0 &= \frac{\mathbf{F}^{t+\Delta t}-\mathbf{F}^{t}}{\Delta t}\\ \left(\mathbf{K}+\mathbf{C}\right)\boldsymbol{\varphi}_1 &= \mathbf{F}^{t}-\left(\mathbf{M}+\tau_r\mathbf{C}\right)\boldsymbol{\varphi}_0\end{aligned} \tag{20}$$

Advantages of the particular solution over the convolution integral can be highlighted as follows: (i) the Green's matrix needs to be computed only once at time $t=\Delta t$ since the particular solution is not dependent of the Green's matrix; (ii) the external heat load vector is performed analytically as long as the heat load shape function is correctly represented, and (iii) an adaptive strategy where the particular solution changes at each time step can be efficiently developed. In fact, the main drawback of the convolution integral lies in the fact that a numerical quadrature rule must be employed, leading to a certain level of numerical error dependent of the qradrature rule. Moreover, Green's matrices at time instants less than Δt are likely to be computed, increasing the overall cost.

3.3 Computation of the Green's function

Applying the Laplace transform to Eqs. (7)-(9) and taking into account the causality principle, which states that the Green's function is zero for $t<\tau$, the following set of equations in the transformed domain arises when an applied impulse is released at time $\tau=0$:

$$\nabla\cdot\left(k\nabla\bar{G}\left(\mathbf{x},\mathbf{y},s\right)\right)+\delta\left(\mathbf{x}-\mathbf{y}\right)=\left(\tau_r\rho cs^2+\left(\rho c+\tau_r w_b c_b\right)s+w_b c_b\right)\bar{G}\left(\mathbf{x},\mathbf{y},s\right)\ \text{in}\ \Omega \tag{21}$$

$$\bar{G}\left(\mathbf{x},\mathbf{y},s\right)=0\ \text{on}\ \Gamma_1 \tag{22}$$

$$k\nabla\bar{G}\left(\mathbf{x},\mathbf{y},s\right)\cdot\mathbf{n}=0\ \text{on}\ \Gamma_2 \tag{23}$$

The classical Galerkin finite element method (Hughes, 1987) when applied to Eqs. (21)-(23) gives the following expression:

$$\begin{aligned}&\int_{\Omega} W^h(\mathbf{x})\left(\tau_r \rho c s^2 + \left(\rho c + \tau_r w_b c_b\right) s + w_b c_b\right) \bar{G}^h\left(\mathbf{x}, \mathbf{y}_j, s\right) d\Omega_{\mathbf{x}} + \\ &\int_{\Omega} \nabla W^h(\mathbf{x}) \cdot k \nabla \bar{G}^h\left(\mathbf{x}, \mathbf{y}_j, s\right) d\Omega_{\mathbf{x}} = \int_{\Omega} W^h(\mathbf{x}) \delta\left(\mathbf{x} - \mathbf{y}_j\right) d\Omega_{\mathbf{x}}\end{aligned} \quad , \; j \in \eta - \eta_{\Gamma_1} \tag{24}$$

where $W^h(\mathbf{x}) = \sum_{i \in \eta - \eta_{\Gamma_1}} N_i(\mathbf{x}) W_i$ stands for the weighting function. Equation (24) can be written in an equivalent matrix form as:

$$\left(\tau_r \mathbf{M} s^2 + \left(\mathbf{M} + \tau_r \mathbf{C}\right) s + \mathbf{C} + \mathbf{K}\right) \bar{\mathbf{g}}_j(s) = \mathbf{1}_j, \quad j \in \eta - \eta_{\Gamma_1} \tag{25}$$

where $\mathbf{1}_j$ denotes a unit base vector and $\bar{\mathbf{g}}_j(s)$ the Green's vector such that the full Green's matrix in the Laplace domain is constructed as $\bar{\mathbf{G}}(s) = \left(\bar{\mathbf{g}}_1(s), \bar{\mathbf{g}}_2(s), \ldots, \bar{\mathbf{g}}_j(s), \ldots\right)$.

The nodal values of the time-dependent Green's function can be obtained from their values in the transformed domain, Eq. (25), by means of an inverse Laplace transform. In the present paper, the Zakian inversion algorithm is employed to find a solution in the time domain. Thus, the inversion of the Green's vector at time $t = \Delta t$, adopting the Zakian algorithm can be written as (recall that the Green's vectors must be computed only once):

$$\mathbf{g}_j(\Delta t) = \frac{2}{\Delta t} \sum_{i=1}^{N/2} \mathrm{Re}\left[k_i \bar{\mathbf{g}}_j\left(\frac{\alpha_i}{\Delta t}\right)\right] \tag{26}$$

where the constants k_i and α_i appear in complex conjugate pairs. It is shown in the numerical example that $N = 2$ is sufficient to yield accurate results. For $N = 2$ the constants are given by $k_1 = -1 + 3.53553390593274i$ and $\alpha_1 = 2 + 1.41421356237309505\mathrm{i}$ (Zakian and Edwards, 1978).

After presenting the way in which the Green's function is computed and bearing in mind the step-by-step time procedure, the hybrid methodology that arises is called ExGA-Zakian.

4 RESULTS AND DISCUSSION

With the objective of showing the applicability and generality of the ExGA-Zakian method to deal with any kind of medium (e.g., homogeneous, heterogeneous, etc.), a triple layer skin model is discussed. The solution is written in terms of the elevated temperature $T_s(\mathbf{x}, t) = T(\mathbf{x}, t) - T_b$ with $T_b = 37^0 C$. The mathematical model is performed considering null initial elevated temperature $T_{s0}(\mathbf{x}) = 0.0^0 C$ subjected to a sudden temperature rise at the skin

surface, with the rest of the boundary considered as adiabatic. A sketch of the model and the finite element mesh constructed with 5179 four-node quadrilateral elements are depicted in Figure 1. It is assumed that, far from skin surface, the tissue is not affected by the prescribed temperature; therefore, a coarse mesh is constructed near the core body. The thermal properties of the skin tissue and the thickness of each layer are given in Table 1. Numerical results obtained by the proposed hybrid time-Laplace technique (i.e., the ExGA-Zakian method) are compared to those of standard FEM formulations employing HHT-α and Crank-Nicolson time-marching schemes (Hughes, 1987).

Layer	**L_i (mm)**	**c ($J.g^{-1}.^0C^{-1}$)**	**k($W.mm^{-1}.^0C^{-1}$)**	**ρ ($g.mm^{-3}$)**	**c_b ($J.g^{-1}.^0C^{-1}$)**	***w_b ($g.mm^{-3}.s^{-1}$)***
Epidermis	$8.0x10^{-2}$	3.6	$2.6x10^{-4}$	$1.2x10^{-3}$	4.2	*0.0*
Dermis	2.0	3.4	$5.2x10^{-4}$	$1.2x10^{-3}$	4.2	$5.0x10^{-7}$
Subcutaneous	*10.0*	*3.06*	$2.1x10^{-4}$	$1.0x10^{-3}$	*4.2*	$5.0x10^{-7}$

Table 1. Thickness and thermal properties for the triple layer skin model.

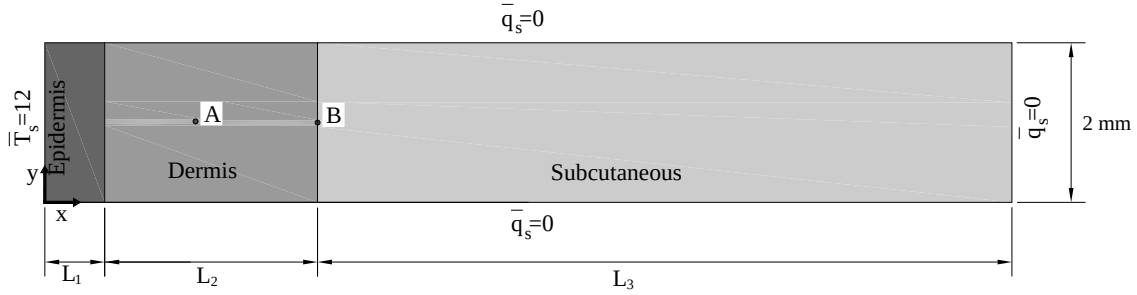

(a)

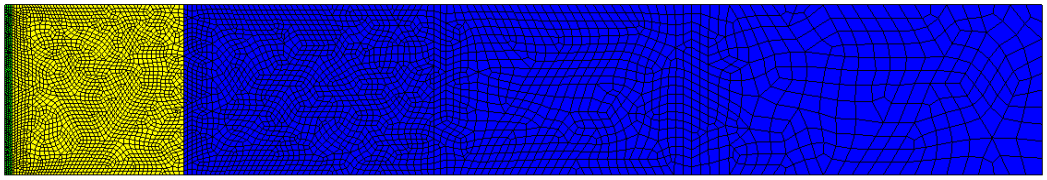

(b)

Figure 1. Heterogeneous biological tissue body: (a) geometry and boundary conditions; (b) domain discretization.

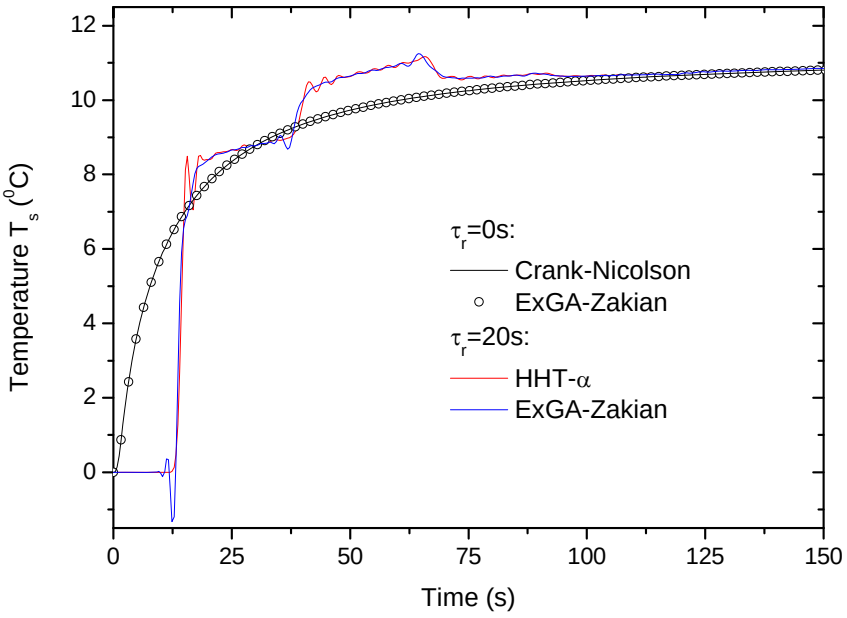

(a)

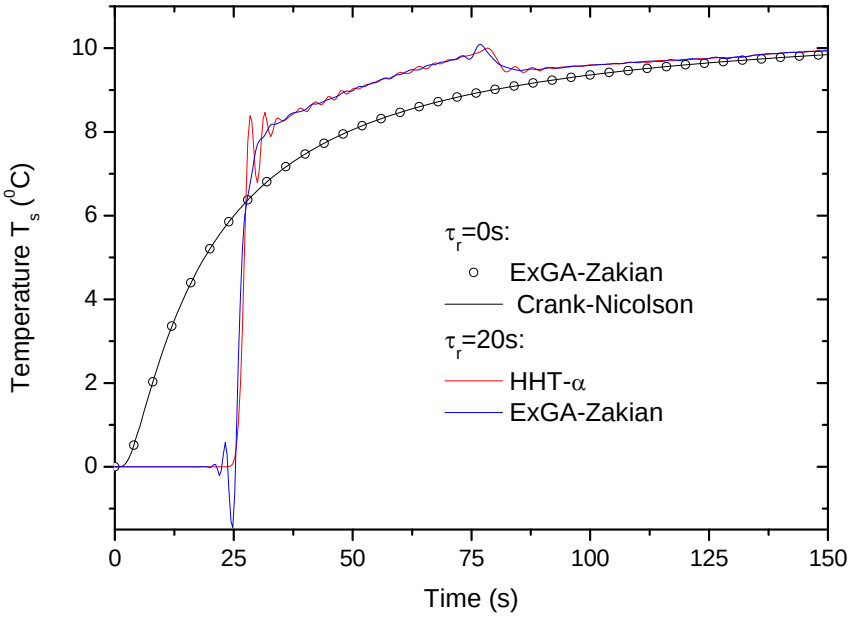

(b)

Figure 2. Comparison of the tissue temperature time-history for $\tau_r = 0s$ and $\tau_r = 20s$ considering the Crank-Nicolson, HHT-α with $\alpha = -1/3$ and ExGA-Zakian schemes using a time step size $\Delta t = 0.4s$: (a) point $A(1.08,1)$; (b) point $B(2.08,1)$.

Time-history results at points $A(1.08,1)$ (dermis layer) and $B(2.08,1)$ (interface between dermis and subcutaneous layers) considering $\tau_r = 0s$ and $\tau_r = 20s$ are shown in Figure 2. It can be seen that the non-homogeneous medium significantly affects the response for $\tau_r = 20s$, where a more complex response is obtained when compared to the parabolic equation, i.e., $\tau_r = 0s$. This is due to superposition effects originated from the reflected thermal waves at the interface between layers. Because of the wave fronts, numerical oscillations near the jumps arise in the hyperbolic model for the HHT and ExGA-Zakian methods, indicating that a more robust methodology should be sought to control these spurious oscillations. Nonetheless, despite the difference of each model, both of them reach the same steady-state solution. The temperature distribution at different time instants, for the parabolic and hyperbolic models, is displayed in Figures 3-4, respectively. It is clearly seen that the temperature distribution for the parabolic model (infinite wave speed) reaches the deeper tissue faster than that of the hyperbolic one (finite wave speed).

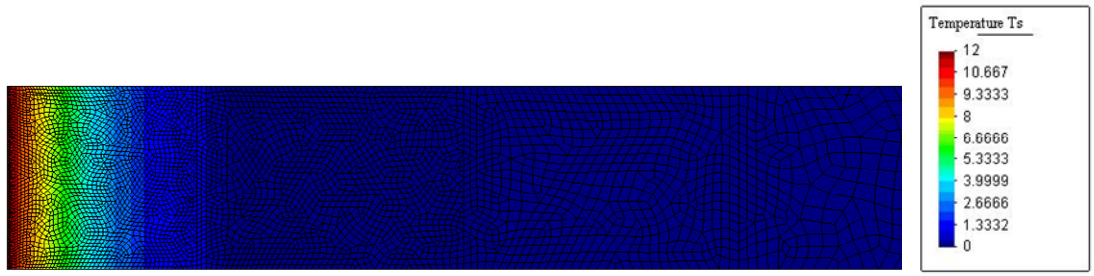

(a)

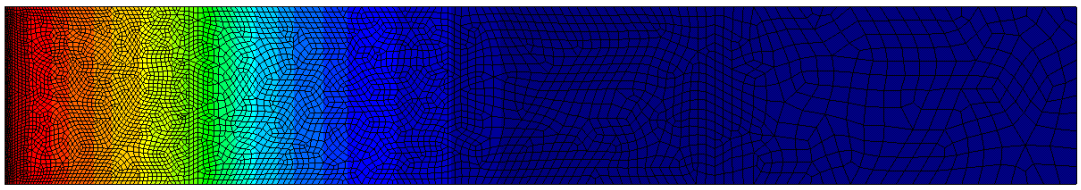

(b)

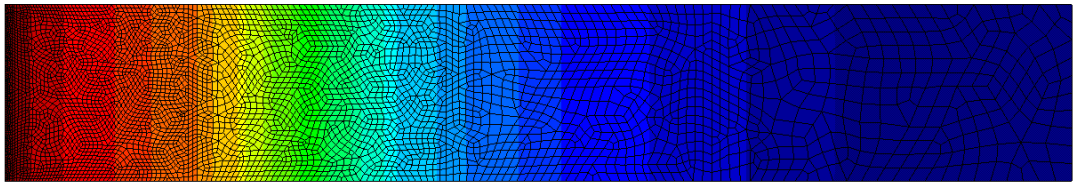

(c)

Figure 3. Tissue temperature field at different time instants for $\tau_r = 0s$ considering the ExGA-Zakian scheme: (a) $t = 4.4s$; (b) $t = 32.4s$; (c) $t = 100.4s$.

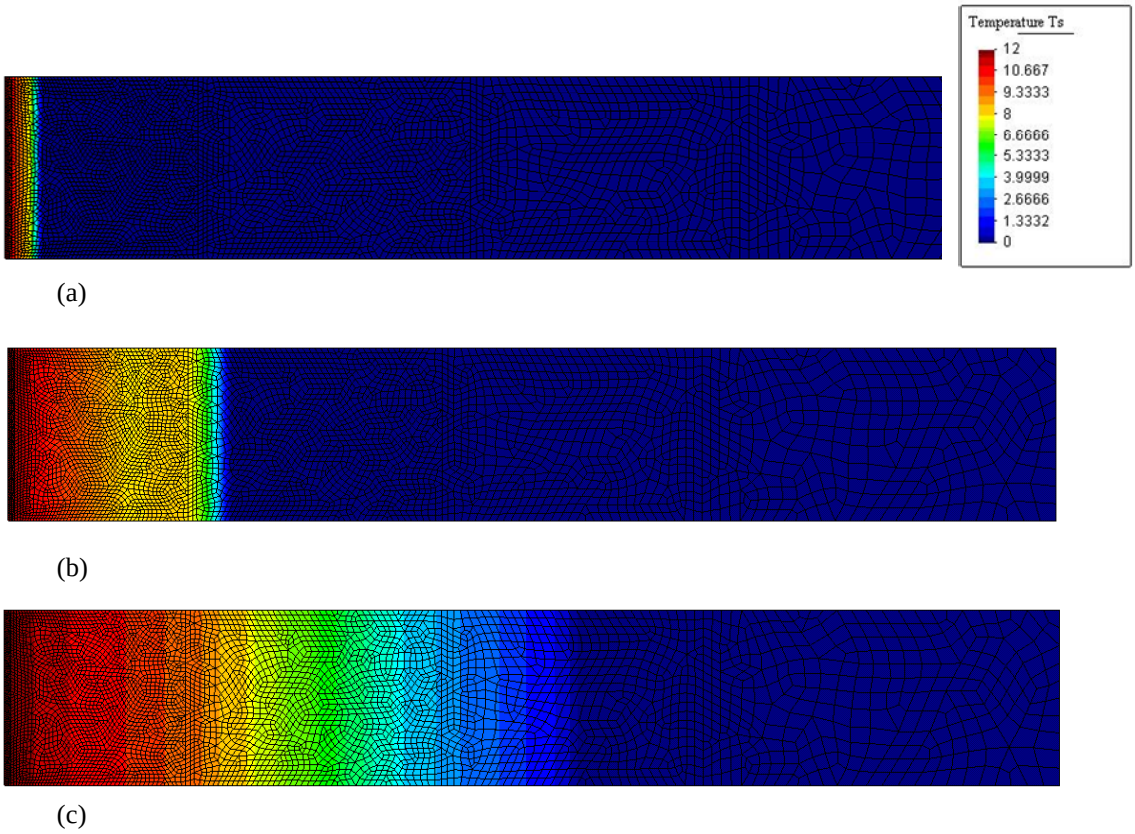

Figure 4. Tissue temperature field at different time instants for $\tau_r = 20s$ considering the ExGA-Zakian scheme: (a) $t = 4.4s$; (b) $t = 32.4s$; (c) $t = 100.4s$.

5 CONCLUSIONS

In this paper, a hybrid time-Laplace domain technique based on numerical Green's functions has been proposed for the solution of parabolic and hyperbolic bioheat transfer models in a unified manner. This terminology comes from the fact that the Green's function is computed taking into account the Laplace domain and then time-domain expressions for the tissue temperature written in a step-by-step way are used to carry out the solution. As a result, the Green function in the time domain needs to be computed only once at the first time step by the Zakian Laplace inversion algorithm. The numerical bioheat model presented here has been shown that accurate and reliable results are furnished by the proposed hybrid method the so called ExGA-Zakian. Furthermore, the difference between the parabolic and hyperbolic equations into bioheat models has been clearly observed. Because of the complex nature of the hyperbolic equation, further studies need to be performed to deal better with oscillations that may arise in some bioheat hyperbolic model due to the presence of wave fronts.

ACKNOWLEDGEMENT

The financial support of CNPQ ("Conselho Nacional de Desenvolvimento Cientifico e Tecnológico") is gratefully acknowledged.

REFERENCES

Hughes T.J.R., The finite element method: linear static and dynamic finite element analysis, Prentice-Hall, Englewood Cliffs, New Jersey, 1987.

Khanafer, K., and Vafai K., Synthesis of mathematical models representing bioheat transport, in Minkowycz W.J., Sparrow E.M. (eds.), Advances in Numerical Heat Transfer, Vol. 3, Taylor & Francis, New York, pp. 1-28, 2009.

Liu J., Chen X., and Xu L.X., New thermal wave aspects on burn evaluation of skin subjected to instantaneous heating, IEEE Trans. *Biomed. Engrg.* 46: 420–428, 1999.

Loureiro F.S., Time integration methods based on the calculation of numerical Green's functions by the finite element method (in Portuguese), *Master's Thesis, UFRJ-COPPE, Rio de Janeiro/RJ Brazil*, 2007.

Loureiro F.S., Mansur W.J., and Vasconcellos C.A.B., A hybrid time/Laplace integration method based on numerical Green's functions in conduction heat transfer, *Comput. Meth. Appl. Mech. Eng.* 198: 2662–2672, 2009a.

Loureiro F.S., and Mansur W.J., An efficient hybrid time-Laplace domain method for elastodynamic analysis based on the explicit Green's approach, *Int. J. Solids and Struct.* 46: 3093-3102, 2009b.

Loureiro F.S., and Mansur W.J., A novel time-marching scheme using numerical Green's functions: A comparative study for the scalar wave equation, *Comput. Meth. Appl. Mech. Eng.*, DOI: 10.1016/j.cma.2009.12.016, 2010.

Mansur W.J., Vasconcellos C.A.B., Zambrozuski N.J.M., and Rotunno Filho O.C., Numerical solution for linear transient heat conduction using an explicit Green's approach, *Int. J. Heat Mass Tran.* 52: 694–701, 2009.

Zakian V., and Edwards M.J., Tabulation of constants for full grade I_{MN} approximants, *Math. Comp.* 32: 519–531, 1978.